1-2009

Molecular Motion and Performance Enhancement of BORAZAN Fluorescent Dyes

Tyler James Morin
Marquette University

Sergey Lindeman
Marquette University, sergey.lindeman@marquette.edu

James R. Gardinier
Marquette University, james.gardinier@marquette.edu

European Journal of Inorganic Chemistry, Vol. 2009, No. 1 (November 25, 2008): 104-110. DOI.

Molecular Motion and Performance Enhancement of BORAZAN Fluorescent Dyes

Tyler J. Morin
Department of Chemistry, Marquette University, Milwaukee, WI
Sergey V. Lindeman
Department of Chemistry, Marquette University, Milwaukee, WI
James R. Gardinier
Department of Chemistry, Marquette University, Milwaukee, WI
First published: 18 December 2008

Abstract

The preparation of three 2,6-dipyrazolyl-4-X-anilines, H(pz_2An^X) (X = *p*-CF_3, Cl, *t*Bu) using CuI-catalyzed amination is described. Subsequent reactions of H(pz_2An^X) with triphenylboron proceeds with benzene elimination to give the corresponding $Ph_2B(pz_2An^X)$ compounds in high yields. The $Ph_2B(pz_2An^X)$ are more highly emissive in the solid state than the previously reported BORAZAN fluorophores, $Ph_2B(pzAn^X)$, their monopyrazolyl counterparts. As with the $Ph_2B(pzAn^X)$, the color of emission in $Ph_2B(pz_2An^X)$ can be tuned simply by varying the *para*-aniline substituent where the emission of

$Ph_2B(pz_2An^X)$ is red-shifted relative to the corresponding $Ph_2B(pzAn^X)$ derivatives. The electronic properties were studied by cyclic voltammetry and electronic absorption/emission spectroscopy as well as by density functional calculations (B3LYP/6-31G*). The di-pyrazolyl derivatives exhibit greater stability toward solvolysis and higher photoluminescent quantum yields (despite the red-shift in emission) compared to their monopyrazolyl counterparts presumably due to kinetic stabilization of the chromophore imparted by the second pyrazolyl ligand. For $Ph_2B(pz_2An^X)$, evidence for intramolecular motion of the diphenylboryl moiety traversing both pyrazolyl groups was detected by variable temperature ^1H NMR spectroscopy. The rate increases with increasing electron-donor abilities of the *para*-aniline substituent.(© Wiley-VCH Verlag GmbH & Co. KGaA, 69451 Weinheim, Germany, 2009)

Abstract

Diphenylboryl complexes of 2,6-bis(pyrazolyl)anilines are more robust and more highly-emissive colour-tuneable fluorophores than derivatives with only one pyrazolyl bound to the aniline ring. Evident from VT-NMR studies, the origin of these favourable characteristics is likely kinetic via promotion of chelate ring formation should dissociation occur.

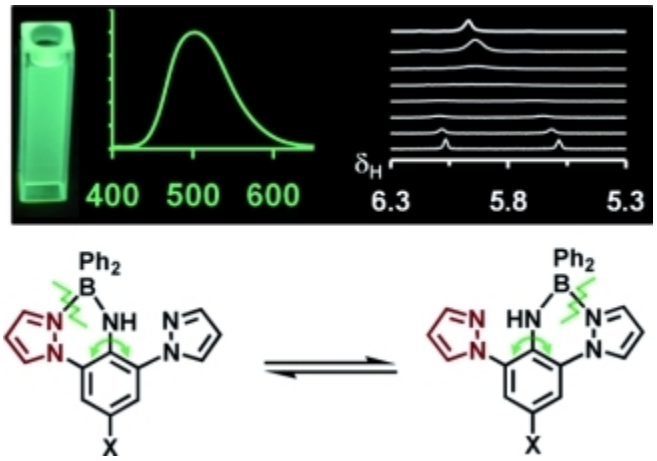

Introduction

There is a longstanding interest in developing new brightly-emitting fluorophores for fundamental studies and for a variety of applications, from sensors and display technology to biomedical imaging.**1** Boron species such as BODIPY™[2] and other N,N-**3** and N,O- chelates**4** have been particularly well-suited for such studies owing to their favourable synthetic protocol, stability, and photophysical properties. We recently reported**5** on a series of colour tuneable fluorescent dyes based on the diphenylboron complexes of (2-pyrazolyl)-4-X-anilines, or BORAZANs (Figure **1**) of the type $Ph_2B(pzAn^X)$ where pz is a pyrazolyl, An is aniline and superscript X is the *para* substituent of the aniline ring. The emission colour, intensity, and reactivity of the fluorescent dyes could be tuned in a regular way by varying the *para*-aniline substituent. For instance, the cyano derivative gave the most intense blue emission [$^{em}\lambda_{max}$ (toluene) = 452nm,Φ_F(toluene) = 0.81] and was the most stable toward solvolysis with protonated solvents such as water or alcohols. The methoxy derivative gave much less intense yellow-green emission [$^{em}\lambda_{max}$ (toluene) = 522 nm, Φ_F (toluene) = 0.07] and readily decomposed in

protic media. The quantum yields of emission were also greatly reduced in aprotic Lewis-basic solvents compared to hydrocarbon solvents. We conjectured that dynamic solution processes may be related to the low quantum yield of emission and the high reactivity of BORAZANS toward Lewis bases. That is, the integrity of the dye would be compromised if boron-pyrazolyl ring dissociation occurred; resulting in lower quantum yields and the resulting three-coordinate boron may provide a pathway for degradation. In order to test this hypothesis, we have modified the dye structure by putting an additional pyrazolyl ring at the 6-position of the aniline (Figure **2**). Such a substitution was designed with the intent of kinetically stabilizing the dye by effectively doubling the rate of boron-pyrazolyl bond formation should boron-pyrazolyl dissociation occur in solution. Moreover, with such a substitution pattern any dynamic processes would be easily detected by NMR, as the pyrazolyl rings would be magnetically inequivalent in a static structure, such as in Figure **2**, but would be equivalent if exchange occurred. We report here on the successful implementation of this structural modification for enhancing the performance of BORAZAN dyes. Moreover, the new ligand may be attractive for the future development of mono- and dimetallic transition metal systems, and the current study provides a basis for evaluating the potential photo- and electrochemical "non-innocence" of this scaffold.

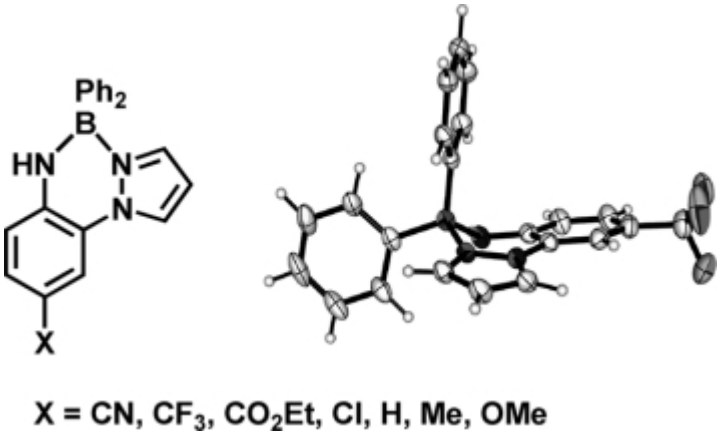

Figure 1. The BORAZAN dye framework and representative solid-state structure of $Ph_2B(pzAn^{CF3})$ from ref.**1**

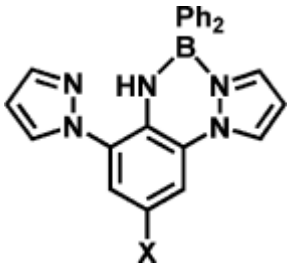

Figure 2. Representation of the 2nd-generation $Ph_2B(pz_2An^X)$ compounds.

Results and Discussion

A summary of the preparative routes to the various ligands and BORAZAN dyes is given in Scheme **1**. The syntheses of the first-generation H(pzAn^{X}) ligands [X = CF_3 (**L1a**), Cl (**L1b**), *t*Bu (**L1c**)] and BORAZAN dyes Ph_2B(pzAn^{X}) [X = CF_3 (**1a**), Cl (**1b**), *t*Bu (**1c**)] follows the literature method (Scheme **1**, a),**5** where **L1c** and **1c** represent new derivatives. The latter were prepared by monobromination of *p-tert*-butylaniline followed by copper-catalyzed amination by the methodology of Buchwald**6** and Taillefer**7** to afford **L1c** which was subsequently converted to **1c** in high yield by reaction with triphenylboron in toluene. The second-generation ligands H(pz_2An^{X}) [X = CF_3 (**L2a**), Cl (**L2b**), *t*Bu (**L2c**)] and BORAZAN dyes $Ph_2B(pz_2An^{X})$ [X = CF_3 (**2a**), Cl (**2b**), *t*Bu (**2c**)] were prepared by an analogous route (Scheme **1**, b) after first di-brominating the appropriate aniline.**8** The subsequent copper-catalyzed amination of the 2,6-dibromo-4-X-aniline required longer reaction times to afford the desired H(pz_2An^{X}) in reasonable yield. The ensuing reaction with triphenylboron proceeded smoothly to afford high yields of the desired **2a**–**2c** with the elimination of benzene.**9**

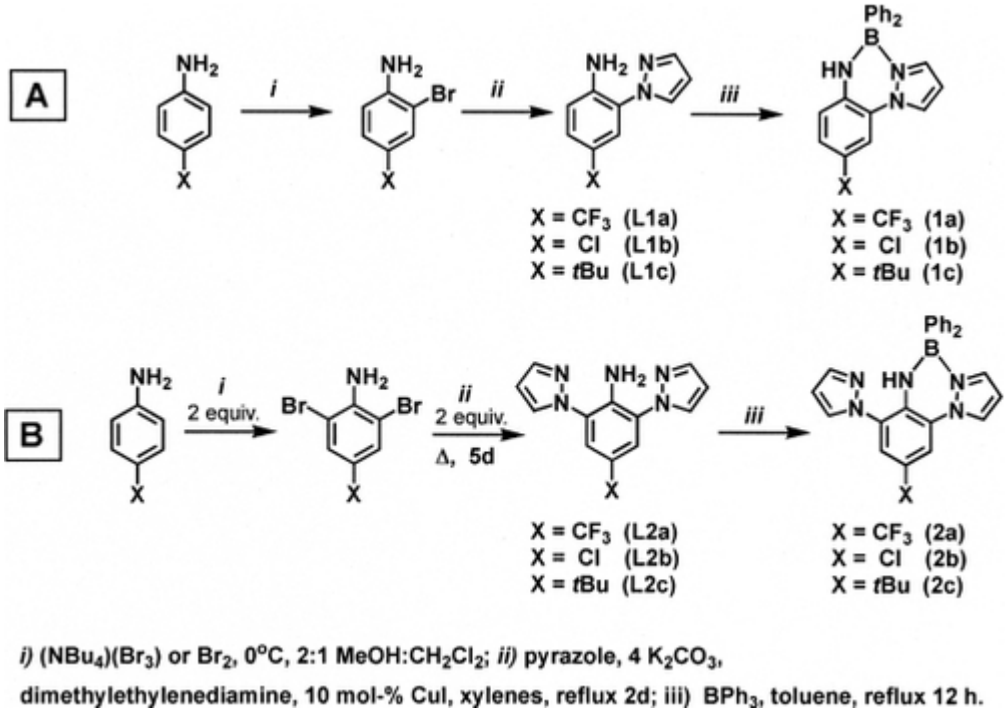

Scheme 1. Preparation of BORAZAN dyes.

The BORAZAN dyes are insoluble in hexanes, **1a**–**1c** are soluble in benzene whereas **2a**–**2c** (based on pz_2An^{X}) are modestly soluble, and all are soluble in toluene, halocarbons, and polar Lewis-basic solvents (THF, CH_3CN, DMF). The compound $Ph_2B(pzAn^{tBu})$ (**1c**) rapidly decomposes (over a period of minutes) in alcohols, as foundpreviously for $Ph_2B(pzAn^{X})$ (X = Me, MeO), but $Ph_2B(pz_2An^{X})$ [X = CF_3 (**2a**), Cl (**2b**), *t*Bu (**2c**)] persist over days in this type of solvent. In addition, the second-generation BORAZAN dyes **2a**–**2c** appear indefinitely air stable in the solid or in solution, in stark contrast to the first generation counterparts **1a**–**1c** which decompose by hydrolysis over time even in the solid state. As further testament to the improved stability of the dyes, the dipyrazolyl derivatives **2a**–**2c** can survive flash chromatography on silica gel, a procedure that immediately annihilates the monopyrazolyl BORAZANs **1a**–**1c**.

The molecular structures of the free ligand H(pz_2An^{tBu}) (**L2c**) and four BORAZAN derivatives $Ph_2B(pzAn^{tBu})$ (**1c**), and $Ph_2B(pz_2An^{X})$ (X = CF_3, Cl, *t*Bu; **2a**–**2c**) have been determined by single-crystal X-ray diffraction. The structures of H(pz_2An^{tBu}) (**L2c**) and its BORAZAN derivative $Ph_2B(pz_2An^{tBu})$ (**2c**) is given in Figure **3** while all other structures, a Table of metrical parameters, and full structural discussion are provided in the Supporting Information. The structure of **L1c** (Figure **3**, a) reveals a pyramidal amino nitrogen (sum of angles around N1 = 341.7°) with hydrogen atoms directed below one face of the aniline ring. The pyrazolyl rings are also directed below the same face with an average dihedral of 43° with respect to the central aniline ring to give relatively long and presumably weak intramolecular hydrogen bonding interactions N1H1b···N12 (2.15 Å, 133°) and N1H1a···N22 (2.20 Å, 133°). In **2c**, the boron-bound pyrazolyl is closer to coplanarity with respect to the central aniline ring (dihedral of 14.1°) whereas the other pyrazolyl is further from coplanarity with a dihedral of 49.3° A feature in **2c** that is common to all other structurally characterized BORAZAN dyes is C_1 (rather than C_s) symmetry due to puckering of the six-member chelate ring into a pseudo half-chair conformation with a distorted tetrahedral boron residing above (0.42 Å) the remaining atoms of the chelate ring As with previously reported members of the BORAZANs, the average B–N distance (1.57 Å) is 0.05 Å shorter than the average B–C distance (1.62 Å) regardless of the substitution pattern along the dye framework. Also, the B–C bond of the axial phenyl is detectably longer (1.62–1.64 Å) than that of the equatorial phenyl (1.61–1.62 Å), presumably due to the anti-bonding interaction involving the anilne moiety (see HOMO in top of Figure **5**).

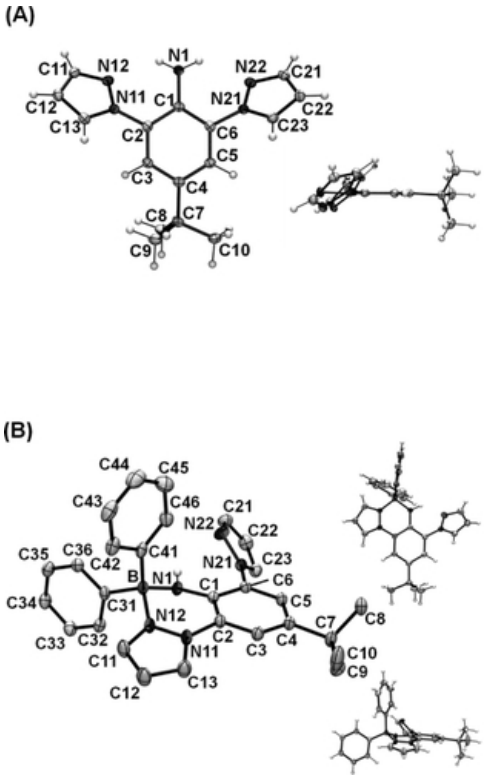

Figure 3 Molecular structure of (A) H(pz_2An^{tBu}) (**L2c**), two views shown. (B) left: $Ph_2B(pz_2An^{tBu})$ (**2c**) with atom labelling and most hydrogen atoms removed for clarity. right: alternate views with hydrogen atoms added. Ellipsoids are shown at the 50 % probability level.

The solution NMR spectra of all BORAZANs [either $Ph_2B(pzAn^X)$ (**1a**–**1c**) or $Ph_2B(pz_2An^X)$ (**2a**–**2c**)] clearly show dynamic processes occur such that their solution structures appear to have higher than the C_1 symmetry indicated from either solid state structural or theoretical studies (vide infra). For instance, only one set of resonances for phenyl ring hydrogen atoms is observed for all theBORAZANs even though, based on the solid-state structures, two sets are expected (one set each for "axial" and "equatorial" phenyls). We previously attributed this observation to a low energy ring-flipping process, that was fast on the NMR time-scale even at –80 °C in [D_8]toluene, a process we still favour after considering the results of variable temperature NMR studies on the $Ph_2B(pz_2An^X)$ series of compounds which showed only one set of phenyl hydrogen resonances at –80 °C. With the $Ph_2B(pz_2An^X)$ series (X = CF_3, Cl, *t*Bu), variable temperature studies also indicate that exchange occurs rendering the boron-bound and "free" pyrazolyl rings inequivalent at low temperatures but equivalent at higher temperatures. As a representative example, a portion of the ^{1}H NMR spectra of $Ph_2B(pz_2An^{tBu})$ (**2c**) in the region showing the resonance(s) for the hydrogen(s) at the 4-position of the pyrazolyl at various temperatures is shown in Figure **4** (X = *t*Bu). More complete ^{1}H NMR spectra for **2c** and other derivatives acquired at different temperatures are collected in the Supporting Information. At –80 °C there are two resonances for 4-pyrazolyl hydrogen atoms at 5.94 and at δ = 5.36 ppm. Comparisons of chemical shifts of the 4-pyrazolyl hydrogen resonances in $Ph_2B(pz_2An^{tBu})$ (**2c**) with those of the related free ligands $H(pzAn^{tBu})$ (**L1c**) (δ_H = 6.11) and $H(pz_2An^{tBu})$ (**L2c**) (δ_H = 6.12) and the monopyrazolyl BORAZAN derivative $Ph_2B(pzAn^{tBu})$ (**1c**) (δ_H = 5.53) establish that the lower field resonance is due to the free pyrazolyl while the higher field resonance is for the boron-bound pyrazolyl. On warming to 0 °C there is a constant downfield shift in both resonances. Above 0 °C the resonances broaden and coalesce at 30 °C, and above the coalescence temperature the single exchange-averaged resonance sharpens. Similar characteristics are shared in the spectra of **2a** and **2b**. The activation barriers for (in hence, the rate of) exchange varies in a regular way with the electron-donating character of the *para*-aniline substituent, as summarized in Table **1**. The more electron-donating substituent gives rise to lower activation barriers and faster rates of exchange. As the activation barrier for exchange falls in line with the expected bond strength of a B–N dative interaction,**10** the mechanism for pyrazolyl exchange, presumably involves pyrazolyl bond dissociation. In this context, electron-withdrawing *para*-aniline substituents render the aniline nitrogen electron-deficient and the nitrogen lone pair is less able to stabilize three-coordinate boron by conjugation with the empty *p*-orbital on boron. The effect is to induce more Lewis-acidic boron and, hence, more stable boron-pyrazolyl bonds.

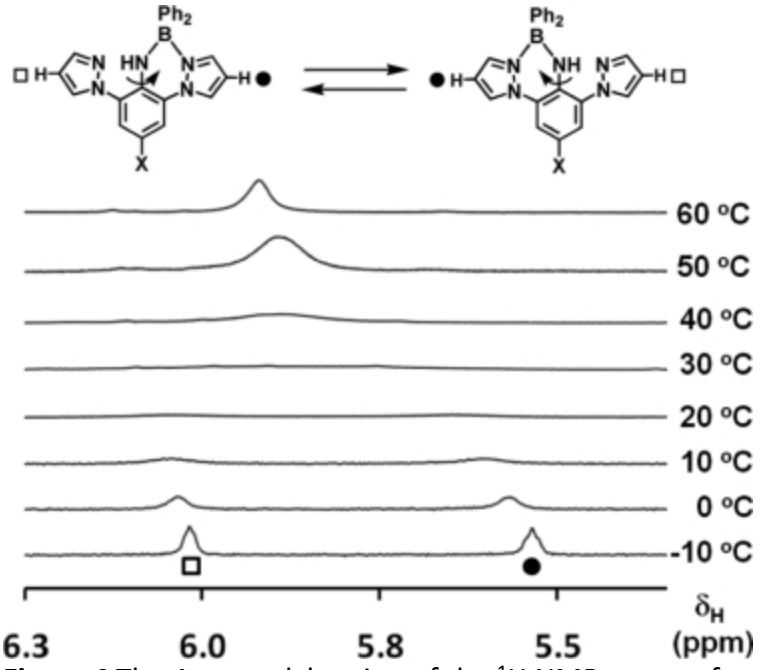

Figure 4 The 4-pyrazolyl region of the ^{1}H NMR spectra for a [D_8]toluene solution of $Ph_2B(pz_2An^{tBu})$ acquired at various temperatures.

Table 1. Activation parameters for pyrazolyl exchange in $Ph_2B(pz_2An^X)$ (X = CF_3, Cl, *t*Bu).

Compound	T_c [K]	$\Delta\nu$ [Hz][a]	k_c [s^{-1}][b]	$\Delta G^{\ddagger}$ [kcal/mol][c]
$Ph_2B(pz_2An^{CF3})$	343	132	586.46	15.8
$Ph_2B(pz_2An^{Cl})$	318	152	675.32	14.5
$Ph_2B(pz_2An^{tBu})$	303	232	1030.75	13.6

[a] Chemical shift difference in the absence of exchange.
[b] Rate constant at coalescence temperature $k_c = \pi\Delta\nu(2)^{-1/2}$.
[c] $\Delta G^{\ddagger} = 4.57(T_c)[10.32 + \log(T_c/k_c)]$ as in reference.11

Density functional calculations (B3LYP/6-31G*,SPARTAN06)**12** were performed on the free ligands $H(pzAn^{tBu})$ (**L1c**), $H(pz_2An^X)$ (**L2a**–**L2c**), and the boron derivatives, $Ph_2B(pz_nAn^X)$ (*n* = 1, 2; X = CF_3, Cl, *t*Bu), **1a**–**1c** and **2a**–**2c**, respectively) using ab initio (HF/321-G) energy-minimized structures in an effort to rationalize the rather unexpected electronic properties of the BORAZAN dyes. The geometry optimization showed good correlation with the solid-state structures in both bond lengths and angles, especially showing chelate ring-puckering as found in the solid state. A representative set of frontier orbitals (HOMO and LUMO) for **2a** is given in the top of Figure **5** while a comparison of energy levels of a more extensive set of frontier orbitals [LUMO(+4) to HOMO(–4)] for all the ligands, $H(pz_nAn^X)$ (*n* = 1, 2; X = CF_3, Cl, *t*Bu) and their corresponding BORAZANs $Ph_2B(pz_nAn^X)$ (*n* = 1, 2) are given in in the bottom of Figure **5**. Complete molecular orbital diagrams are provided in the Supporting Information. For all, the HOMO is mainly the nonbonding representation of the aniline-centred pi-system, encompassing the nitrogen-centered lone pair of the aniline.

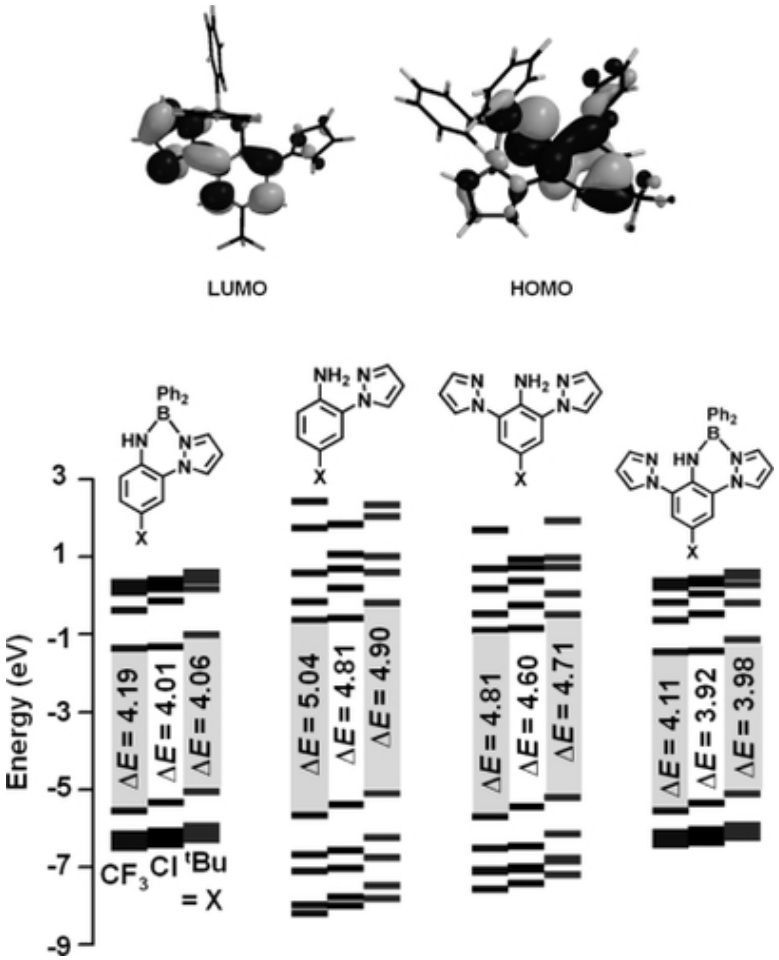

Figure 5. Top: HOMO and LUMO for representative complex **2a**. Bottom: comparison of the energy levels of frontier orbitals LUMO(+4) to HOMO(–4) for H(pz_nAn^X) (*n* = 1, 2) and corresponding BORAZANs $Ph_2B(pz_nAn^X)$ (*n* = 1, 2) where X = CF_3, Cl, and *t*Bu (left to right) for each compound type from density functional calculations (B3LYP/6-31G*). Vertical scale represents relative energy. Gas-phase HOMO–LUMO gap energy is Δ*E*.

There is also a significant (pi-antibonding) contribution from the orbitals of the *para*-aniline substituent to the HOMO. Following the convention established by from the seminal work of Kasha and Rawls on the photophysics of aniline derivatives,**13** it is convenient to refer to the HOMO (and other frontier orbitals containing significant contributions from the conjugated aniline lone pair) as a π_L (pi-lone-pair) to provide a distinction from a pure π orbital. Deviations from aniline nonplanarity such as twisting of the H_2N-aryl moiety about C–N bond (or other distortions) change the photophysics of the molecule by affording more nonbonding character to the nitrogen lone pair. The LUMO of each compound is π* in character and spans the pi-systems of both the aniline and the pyrazolyl rings with only a small contribution from the conjugated *p*-orbital of the aniline nitrogen. For the H(pz_nAn^X) (*n* = 1,2) ligands, the HOMO(–4) to HOMO(–1) orbitals are π-bonding, the virtual orbitals LUMO (+1) to LUMO(+3) are π* anti-bonding, while the LUMO(+4) and higher are σ* anti-bonding. In the $Ph_2B(pz_nAn^X)$ (*n* = 1,2), orbital contributions from the diphenylboron moiety distinguish the BORAZANs from the ligands. The HOMO(–1) to HOMO(–4), are essentially four linear combinations of boron-phenyl π-orbitals; the next-lowest pzAn-based π_L-orbital is HOMO(–5). The corresponding four π* orbitals include contributions

from both the pzAn and diphenylboryl moieties and constitute the virtual orbitals LUMO(+1) to LUMO(+5).

The relative energies of the frontier orbitals for the twelve compounds in the bottom of Figure **5** (and Supporting Information) reveals a number of trends that correlate well with experimental data. When comparing the relative energy of the HOMO of a given H(pzAn^X) ligand with that for its corresponding BORAZAN (Figure **5**), the latter is destabilized owing to an antibonding pi-interaction between the boron-bound carbon atoms and the *p*-orbital of the aniline nitrogen, which is not present in the former. There is a stabilization of the HOMO with an increase in electron-withdrawing character of the *para* substituent of the aniline, rendering the aniline a poorer donor, as expected. Contrary to initial expectations based solely on inductive effects, substitution of the *ortho* hydrogen with a pyrazolyl results in a small stabilization of the HOMO that arises due to increased conjugation with the pi-system of the new pyrazolyl group. This increase in conjugation for the dipyrazolyl system causes a significant stabilization of the LUMO, which results in an overall smaller HOMO/LUMO energy gap compared to the monopyrazolyl systems. As with the monopyrazolyl systems the HOMO is destabilized to a greater extent than the LUMO is stabilized on changing *para*-aniline substituents, which provides an additional basis for tuning the electronic properties of the BORAZAN dyes.

Electrochemistry

As aniline derivatives are well known electron donors,**14** and BORAZAN derivatives were previously found to be electroactive,**5** the electrochemistry of CH_3CN solutions of the new ligands and BORAZANs were examined by cyclic voltammetry. The electrochemical data are collected in Table **2** while voltammograms for the ligands and complexes are found in the Supporting Information. Each of the compounds exhibited an irreversible oxidation in the range of 0.7–1.4 V (vs. Ag/AgCl), where the reported potentials are those for the anodic wave observed at a scan rate of 0.100 V/s; the cathodic wave is either absent or noticeably less intense than expected. For each series of ligands and BORAZANs, the oxidation becomes more favourable with increasing electron donating character of the *para*-aniline substituent, in accord with previous findings and with the calculations that showed a destabilization of the HOMO for such substitution. Thus, for the $BPh_2(pz_2An^X)$, the oxidation potentials increase along the series X = *t*Bu (E_{pa} = 0.86 V) < X = Cl (E_{pa} = 1.10 V) < X = CF_3 (E_{pa} = 1.13 V). Also in agreement with calculations and earlier results, the oxidations of the BORAZAN complexes are more favourable than those for the free ligands because there is a destabilization of the HOMO brought about by antibonding interactions with the σ-orbitals of the boron-bound carbon atoms. The dipyrazolyl derivatives (both free ligands and BORAZAN complexes) are more difficult to oxidize than the monopyrazolyl analogues. Thus, the oxidation potentials for the series $Ph_2B(pz_2An^X)$ [X = CF_3 (1.13 V), Cl (1.10 V), *t*Bu (0.86 V)] are higher than the corresponding potentials for the $Ph_2B(pzAn^X)$ series [X = CF_3, (1.04 V), Cl (0.84 V), *t*Bu (0.74 V)]. While this result is surprising on first inspection considering the expected inductive effects of replacing hydrogen with a more electron-donating pyrazolyl, this trend was correctly predicted by the calculations, which showed that the origin is due to stabilization of the HOMO via conjugation with the pi-orbitals of the second pyrazolyl.

Table 2. Electronic properties of various pyrazolylaniline ligands and diphenylboryl complexes.

Compound	**$E_{1/2}$ (V vs. Ag/AgCl)[a]**		**Absorption[d]**	**Emission[d]**		**Ref.**

	Oxidation[b]	Reduction[c]	λ_{max} (ϵ, M^{-1} cm^{-1}), CH_2Cl_2	λ_{max}^{em} (nm)	Φ_F (C_7H_8, CH_3CN)	
H(pzAn^{CF3}), **L1a**	1.23	–	234 (21,000), 259 (8,600), 305 (3,700)	–	–	**2**
H(pzAn^{Cl}), **L1b**	1.01	–	233 (24,000), 255 (9,600), 317 (4,700)	–	–	**2**
H(pzAn^{tBu}), **L1c**	0.88	–	234 (17,825), 251sh (7,252), 305 (3,755)	–	–	[e]
H(pz$_2$An^{CF3}), **L2a**	1.41	–2.60	237 (24,971), 259sh (7,135), 310 (5,049)	–	–	[e]
H(pz$_2$An^{Cl}), **L2b**	1.24	–2.50	240 (24,814), 263sh (5,109), 329 (4,369)	–	–	[e]
H(pz$_2$An^{tBu}), **L2c**	0.99	–	229 (26,464), 262sh (6,935), 315 (5,433)	–	–	[e]
Ph$_2$B(pzAn^{CF3}), **1a**	1.04	–2.39	248 (31,000), 288 (13,000), 358 (4,700)	468	0.66, 0.49	**2**
Ph$_2$B(pzAn^{Cl}), **1b**	0.84	–2.41	249 (32,000), 289 (7,800), 375 (6,600)	481	0.44, 0.23	[e]
Ph$_2$B(pzAn^{tBu}), **1c**	0.74	–2.64	245 (32,251), 371 (4,853)	495	0.33, 0.03	[e]
Ph$_2$B(pz$_2$An^{CF3}), **2a**	1.13	–2.43	252 (30,016), 292 (6,500), 372 (6,359)	474	0.75, 0.55	[e]
Ph$_2$B(pz$_2$An^{Cl}), **2b**	1.10	–2.58	251 (26,768); 289sh (3,528); 388 (5,460)	493	0.53, 0.31	[e]
Ph$_2$B(pz$_2$An^{tBu}), **2c**	0.86	–2.65	247 (28,505), 380 (5,706)	502	0.46, 0.16	[e]

[a] Scan rate of 100 mV/s in CH_3CN with $NBu_4(PF)_6$ as supporting electrolyte.
[b] Anodic peak potential.
[c] Cathodic peak potential.
[d] 295 K, CH_2Cl_2.
[e] This work.

Electronic Spectra

The electronic (absorption/emission) spectra of the newly prepared H(pz$_n$An^X) ligands and Ph$_2$B(pz$_n$An^X) (n = 1,2; X = CF_3, Cl, *t*Bu) compounds parallel those of the previously reported monopyrazolyl (n = 1; X = CF_3, Cl) derivatives. A summary of the electronic properties are collected in Table **2** and complete spectra are found in the Supporting Information. The electronic absorption spectrum of each H(pz$_n$An^X) (n = 1,2) ligand consists of three bands for π-π* transitions; one high-intensity, high-energy band at ca. 230 nm ($\epsilon \approx 20{,}000$), a second less intense band at ca. 250 ($\epsilon \approx 7000$) nm (in some cases this band occurs as a shoulder to the high-energy band),and a low-energy, low-intensity band for the π_L–π* (HOMO–LUMO) transition above about 300 nm ($\epsilon \approx 3000$). As indicated from the calculations, the energies of all the absorption bands of the dipyrazolyl derivatives are red-shifted with respect to the monopyrazolyl derivatives. With the BORAZANs, each band undergoes both hyper- and bathochromic

shifts and a new high energy band (presumably for the π–π* transitions involving the boron-phenyl groups) appears as a shoulder near 200 nm.

The ligands are not emissive under irradiation with UV-light but the BORAZANs exhibit intense emission (either in the solid state or in hydrocarbon or halocarbon solution) that varies from blue for derivatives with electron-withdrawing trifluoromethyl *para*-aniline substituents to green for the *tert*-butyl derivatives (Figure **6**). Previous excited-state lifetime measurements of $Ph_2B(pzAn^X)$ (X = CN, CF_3, CO_2Et, Cl, Me, OMe) established the fluorescent nature(ns lifetimes) of emission. As with the previously reported monopyrazolyl derivatives, the emission of the di-pyrazolyl derivatives $Ph_2B(pz_2An^X)$ (X = CF_3, Cl, *t*Bu) exhibit a regular red-shift of emission with increasing electron-donating character of the *para*-aniline substituent. Thus, the emission maximum of $Ph_2B(pz_2An^X)$ occurs at λ_{max}^{em} 474, 493, and 502 nm for X = CF_3 (**2a**), Cl (**2b**), and *t*Bu (**2c**), respectively. The quantum yields of emission diminish regularly along the series X = CF_3, Cl, *t*Bu (0.75, 0.53, 0.46 respectively) in accord with the energy gap law which delineates that quantum yields for emission will decrease with lower energy emission.**15** After considering the implications of the energy gap law, there is a remarkable improvement in the quantum yields of emission of **2a**–**2c** vs. the corresponding monopyrazolyl derivatives **1a**–**1c**. That is, despite the fact that di-pyrazolyl derivatives **2a**–**2c** exhibit red-shifted emission compared to **1a**–**1c** (Supporting Information), the former enjoy a 10–20 % increase in fluorescence quantum yield (Table **2**) with respect to the latter. We tentatively attribute the improvement in quantum yield to the kinetic stabilization of the dye framework brought about by the additional pyrazolyl (increasing the amount of chelated boron) which is supported by the observation that the Stokes shift (6000 ± 500 cm^{-1}) in toluene is slightly smaller for the dipyrazolyl derivatives compared to that observed for the monopyrazolyl derivatives (Stokes shift 6400 ± 500 cm^{-1}). Moreover, the fluorescent quantum yields for **2a**–**2c** in CH_3CN are lower than in toluene but are higher than for analogous **1a**–**1c** in the Lewis-base solvent. As with the previously reported derivatives, the efficacy of fluorescence quenching of **2a**–**2c** in acetonitrile most greatly affects derivatives with electron-rich *para*-aniline substituents [with weaker (or less inert) boron-pyrazolyl dative bonds]. Acetonitrile could be envisioned to coordinate the Lewis-acidic boron centers in the dyes, compromising the integrity of the chelate ring and destroying the chromophore. The bis(pyrazolyl)aniline ligand scaffolds appear to offer a greater resistance to such a degenerative process compared to mono(pyrazolyl)aniline derivatives.

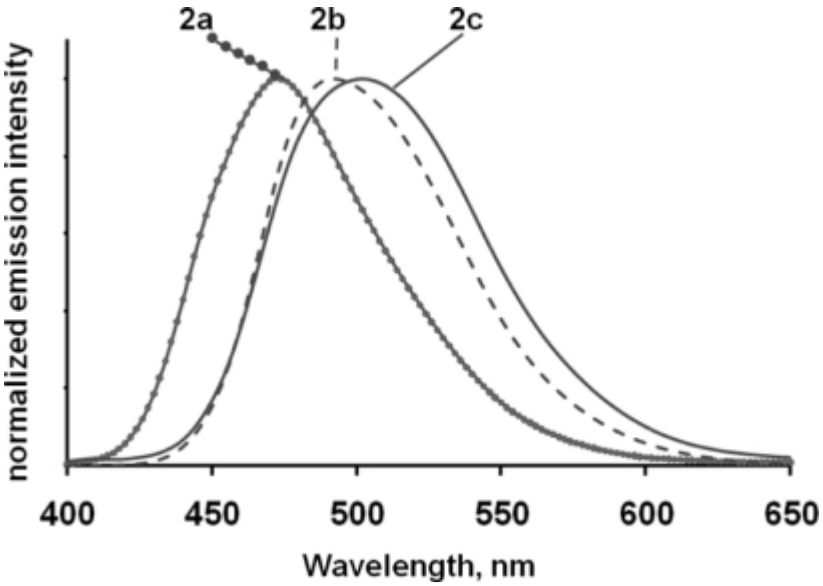

Figure 6. Overlay of normalized emission spectra of $Ph_2B(pz_2An^X)$ where (X = CF_3, **2a** left beaded line; X = Cl, **2b** centre dashed line; X = *t*Bu, **2c** right solid line).

Conclusions

Three examples of 2,6-dipyrazolylanilines $H(pz_nAn^X)$ (X = CF_3, Cl, *t*Bu) have been prepared by exploiting copper-catalyzed amination reactions between pyrazole and 2,6-dibromoaniline. The reaction chemistry of these derivatives with triphenylboron afforded $Ph_2B(pz_2An^X)$ [X = CF_3 (**2a**), Cl (**2b**), *t*Bu (**2c**)] with chelated diphenylboryl moieties, as indicated by X-ray structural studies. These new highly emissive compounds exhibit a number of adventitious properties compared to the first generation of BORAZAN fluorescent dyes, $Ph_2B(pzAn^X)$ [X = CF_3 (**1a**), Cl (**1b**), *t*Bu (**1c**)], that have only one pyrazolyl group on the heterocyclic ligand scaffold. The emission of the new di-pyrazolyl BORAZANs is colour-tuneable from blue for the derivative with an electron-withdrawing –CF_3 *para*-aniline substituent to green for the derivative with a *tert*-butyl substituent, where the emission of the dipyrazolyl derivatives **2a**–**2c** are lower in energy than the corresponding monopyrazolyl derivatives **1a**–**1c**. Despite exhibiting lower energy emissions, the di-pyrazolyl BORAZANs display higher luminescence quantum yields than monopyrazolyl analogues. Moreover, the di-pyrazolyl derivatives enjoy a significant increase in stability towards solvolysis relative to their monopyrazolyl counterparts. Both of the above properties are thought to arise from a kinetic stabilization of the dye framework brought about by the additional pyrazolyl group that could favour an increased rate of boron-pyrazolyl bond formation should dissociation occur. In fact, such dissociation was easily detected by variable-temperature NMR spectroscopic studies of toluene solutions of C_1-symmetric **2a**–**2c** since the resonances for “free” and boron-bound pyrazolyl groups undergo exchange. The rates of boron-pyrazolyl dissociation decrease (hence, the stability of the chelate ring increases) in the order *t*Bu > Cl > CF_3, an order that may be indicative of the anticipated (in)ability of the aniline to stabilize a three-coordinate boron by conjugation between the aniline lone pair and the empty *p*-orbital on boron. We are further probing the reaction chemistry of these new ligands towards transition metals and for the construction of supramolecular assemblies.

CCDC-CCDC-698323 **http://www.ccdc.cam.ac.uk/cgi-bin/catreq.cgi** (for $Ph_2B(pzAn^{tBu})$ **1c**), -CCDC-698324 **http://www.ccdc.cam.ac.uk/cgi-bin/catreq.cgi** (for $H(pz_2An^{tBu})$ **L2c**), -CCDC-698325 **http://www.ccdc.cam.ac.uk/cgi-bin/catreq.cgi** (for $Ph_2B(pz_2An^{CF3})$ **2a**), -CCDC-698326 **http://www.ccdc.cam.ac.uk/cgi-bin/catreq.cgi** (for $Ph_2B(pz_2An^{Cl})$ **2b**), -CCDC-698327 **http://www.ccdc.cam.ac.uk/cgi-bin/catreq.cgi** (for $Ph_2B(pz_2An^{tBu})$ **2c**), and -CCDC-698328 **http://www.ccdc.cam.ac.uk/cgi-bin/catreq.cgi** (for $(Ph_2B)_2(pz_2An^{tBu})$ **3c**) contain the supplementary crystallographic data for this paper. These data can be obtained free of charge from The Cambridge Crystallographic Data Centre via www.ccdc.cam.ac.uk/data_request/cif.

Supporting Information (see also the footnote on the first page of this article): Complete experimental details. Details of X-ray crystallographic studies, tables of X-ray data, molecular and supramolecular structural discussion, NMR spectra, cyclic voltammograms, UV/Vis and emission spectra, details of computational studies, comparison of results from different basis sets, frontier orbital diagrams.

Acknowledgements

J. R. G. thanks Marquette University, the Petroleum Research Fund (74371-G), and the National Science Foundation (NSF) (CHE-0521323) for support.

References

1a. B. Valeur , *Molecular Fluorescence, Principles and Applications*, Wiley-VCH, New York, 2002 . 1b. J.-P. Desvergne , A. W. Czarnik (Eds.), *Chemosensors of Ion and Molecule Recognition*, Kluwer, Dordrecht, The Netherlands, 1997 .

2a. A. Loudet , K. Burgess , Chem. Rev. 2007 , **107** , 4891 – 4932 . 2b. R. P. Haugland , H. C. Kang , U. S. Patent 4 , 774, 339, 1988 . 2c. R. P. Haugland , *Handbook of Fluorescent Probes and Research Chemicals*, 6th ed., Molecular Probes, Eugene, OR, 1996 . 2d. A. Treibs , F.-H. Kreuzer , Justus Liebigs Ann. Chem. 1968 , **718** , 208 – 223 . 2e. J. H. Boyer , A. M. Haag , G. Sathyamoorthi , M. L. Soong , K. Thangaraj , T. G. Pavlopoulos , Heteroat. Chem. 1993 , **4** , 39 – 49 . 2f. G. Beer , C. Niederalt , S. Grimme , J. Daub , Angew. Chem. Int. Ed. 2000 , **39** , 3252 – 3255 . 2g. M. Kollmannsberger , K. Rurack , U. Resch-Genger , J. Daub , J. Phys. Chem. A 1998 , **102** , 10211 – 10220 . 2h. M. Kollmannsberger , T. Gareis , S. Heinl , J. Breu , J. Daub , Angew. Chem. Int. Ed. Engl. 1997 , **36** , 1333 – 1335 . 2i. L. Zeng , E. W. Miller , A. Pralle , E. Y. Isacoff , C. J. Chang , J. Am. Chem. Soc. 2006 , **128** , 10 – 11 . 2j. S. Hattori , K. Ohkubo , Y. Urano , H. Sunahara , T. Nagano , Y. Wada , N. V. Tkachenko , H. Lemmetyinen , S. Fukuzumi , J. Phys. Chem. B 2005 , **109** , 15368 – 15375 . 2k. H. Imahori , H. Norieda , H. Yamada , Y. Nishimura , I. Yamazaki , Y. Sakata , S. Fukuzumi , J. Am. Chem. Soc. 2001 , **123** , 100 – 110 . 2l. R. W. Wagner , J. S. Lindsey , Pure Appl. Chem. 1996 , **68** , 1373 – 1380 .

3. For example: 3a. S. O. McDonnell , D. F. O'Shea , Org. Lett. 2006 , **8** , 3493 – 3496 . 3b. T.-R. Chen , R.-H. Chien , M.-S. Jan , A. Yeh , J.-D. Chen , J. Organomet. Chem. 2006 , **691** , 799 – 804 . 3c. Q. D. Liu , M. S. Mudadu , R. Thummel , Y. Tao , S. Wang , Adv. Funct. Mater. 2005 , **15** , 143 – 154 . 3d. H.-Y. Chen , Y. Chi , C.-S. Liu , J.-K. Yu , Y.-M. Cheng , K.-S. Chen , P.-T. Chou , S.-M. Peng , G.-H. Lee , A. J. Carty , S.-J. Yeh , C.-T. Chen , Adv. Funct.

Mater. 2005 , **15** , 567 – 574 . 3e. N. G. Park , J. E. Lee , Y. H. Park , Y. S. Kim , Synth. Met. 2004 , **145** , 279 – 283 . 3f. G. M. Kaplan , A. N. Frolov , N. I. Rtishchev , A. V. El'tsov , Zhur. Org. Khim. 1991 , **27** , 872 – 877 . 3g. G. M. Kaplan , A. N. Frolov , N. I. Rtishchev , A. V. El'tsov , T. K. Ponomareva , Zhur. Obsch. Khim. 1991 , **61** , 1810 – 1814 . 3h. Y. Cui , Q.-D. Liu , D. R. Bai , W.-L. Jia , Y. Tao , S. Wang , Inorg. Chem. 2005 , **44** , 601 – 609 .

4a. F. P. Macedo , C. Gwengo , S. V. Lindeman , M. D. Smith , J. R. Gardinier , Eur. J. Inorg. Chem. 2008 , 3200 – 3211 . 4b. Y. Qin , Y. Kiburu , S. Shah , F. Jäkle , Macromolecules 2006 , **39** , 9041 – 9048 . 4c. Y. Qin , Y. Kiburu , S. Shah , F. Jäkle , Org. Lett. 2006 , **8** , 5227 – 5230 .

5. B. J. Liddle , R. M. Silva , T. J. Morin , F. P. Macedo , R. Shukla , S. V. Lindeman , J. R. Gardinier , J. Org. Chem. 2007 , **72** , 5637 – 5646 .

6. J. C. Antilla , J. M. Baskin , T. E. Barder , S. L. Buchwald , J. Org. Chem. 2004 , **69** , 5578 – 5587 .

7a. H.-J. Cristau , P. P. Cellier , J.-F. Spindler , M. Taillefer , Eur. J. Org. Chem. 2004 , 695 – 709 . 7b. M. Taillefer , N. Xia , A. Ouali , Angew. Chem. Int. Ed. 2007 , **46** , 934 – 936 . 7c. H.-J. Christau , P. P. Cellier , J.-F. Spindler , M. Taillefer , Chem. Eur. J. 2004 , **10** , 5607 – 5622 . 7d. H.-J. Christau , P. P. Cellier , J.-F. Spindler , M. Taillefer , Eur. J. Org. Chem. 2004 , 695 – 709 . 7e. See also, J. M. Lindley , I. M. McRobbie , O. Meth-Cohn , H. Suschitzky , J. Chem. Soc. Perkin Trans. 1 1980 , **4** , 982 – 994 .

8a. M. Austin , O. J. Egan , R. Tully , A. C. Pratt , Org. Biomol. Chem. 2007 , **5** , 3778 – 3786 . 8b. Q. Zhang , Y. Peng , W. J. Welsh , Heterocycles 2006 , **68** , 2635 – 2645 . 8c. S. H. Lee , B.-B. Jang , Z. H. Kafafi , J. Am. Chem. Soc. 2005 , **127** , 9071 – 9078 . 8d. T. C. Bedard , J. S. Moore , J. Am. Chem. Soc. 1995 , **117** , 10662 – 10671 . 8e. Y. Miura , H. Oka , M. Momoki , Synthesis 1995 , 1419 – 1422 . 8f. A. R. Hajipour , H. Imanieh , S. A. Pourmousavi , Synth. Commun. 2004 , **34** , 4597 – 4604 . 8g. F. Toda , J. Schmeyers , Green Chem. 2003 , **5** , 701 – 703 . 8h. C. Popeney , Z. Guan , Organometallics 2005 , **24** , 1145 – 1155 . 8i. C. Koradin , W. Dohle , A. L. Rodriguez , B. Schmid , P. Knochel , Tetrahedron 2003 , **59** , 1571 – 1587 .

9. It was possible to isolate a few crystals of a side product $(Ph_2B)_2(\mu\text{-}pz_2An^{tBu})$ **3c** (see structure in the Supporting Information). As of yet, the intentional synthesis of **3c** has been hampered by poor reproducibility and/or high reactivity. We are currently pursuing reliable preparations of this and other dinuclear species, which will be the subjects of a future report.

10a. P. D. Livant , D. J. D. Northcott , Y. Shen , T. R. Webb , J. Org. Chem. 2004 , **69** , 6564 – 6571 . 10b. T. M. Gilbert , J. Phys. Chem. A 2004 , **108** , 2550 – 2554 .

11. H. Kessler , Angew. Chem. Int. Ed. Engl. 1970 , **9** , 219 – 235 .

12a. Y. Shao , L. F. Molnar , Y. Jung , J. Kussmann , C. Ochsenfeld , S. T. Brown , A. T. B. Gilbert , L. V. Slipchenko , S. V. Levchenko , D. P. O'Neill , R. A. DiStasio Jr., R. C. Lochan , T. Wang , G. J. O. Beran , N. A. Besley , J. M. Herbert , C. Y. Lin , T. Van Voorhis , S. H. Chien , A. Sodt , R. P. Steele , V. A. Rassolov , P. E. Maslen , P. P. Korambath , R. D. Adamson , B. Austin , J. Baker , E. F. C. Byrd , H. Dachsel , R. J. Doerksen , A. Dreuw , B. D. Dunietz , A. D. Dutoi , T. R. Furlani , S. R. Gwaltney , A. Heyden , S. Hirata , C.-P. Hsu , G. Kedziora , R. Z. Khalliulin , P. Klunzinger , A. M. Lee , M. S. Lee , W. Z. Liang , I. Lotan , N. Nair , B. Peters , E. I. Proynov , P. A. Pieniazek , Y. M. Rhee , J. Ritchie , E. Rosta , C. D. Sherrill , A. C. Simmonett , J. E. Subotnik , H. L. Woodcock III , W. Zhang , A. T. Bell , A. K. Chakraborty , D. M. Chipman , F. J. Keil , A. Warshel , W. J. Hehre , H. F. Schaefer , J. Kong , A. I. Krylov , P. M. W. Gill , M. Head-Gordon , Phys. Chem. Chem. Phys. 2006 , **8** , 3172 – 3191 . 12b. W. J. Hehre , *A Guide to Molecular Mechanics and Quantum Chemical Calculations*, 2nd ed., Wavefunction, Inc., Irvine, CA, 2006 .

13. M. Kasha , R. Rawls , Photochem. Photobiol. 1968 , **7** , 561 – 569 .
14a. Z. Galus , R. N. Adams , J. Phys. Chem. 1963 , **67** , 862 – 866 . 14b. J. Bacon , R. N. Adams , J. Am. Chem. Soc. 1968 , **90** , 6596 – 6599 . 14c. R. L. Hand , R. F. Nelson , J. Am. Chem. Soc. 1974 , **96** , 850 – 860 . 14d. A. G. MacDiarmid , A. J. Epstein , Faraday Discuss. Chem. Soc. 1989 , **88** , 317 – 332 . 14e. A. G. MacDiarmid , Angew. Chem. Int. Ed. 2001 , **40** , 2581 – 2590 . 14f. A. J. Heeger , Angew. Chem. Int. Ed. 2001 , **40** , 2591 – 2611 . 14g. L. R. Sharma , A. K. Manchanda , G. Singh , R. S. Verma , Electrochim. Acta 1982 , **27** , 223 – 233 . 14h. D. G. H. Daniels , F. T. Naylor , B. C. Saunders , J. Chem. Soc. 1951 , 3433 – 3435 .
15a. J. V. Caspar , B. P. Sullivan , E. M. Kober , T. J. Meyer , Chem. Phys. Lett. 1982 , **91** , 91 – 95 . 15b. A. P. Penner , W. Siebrand , M. Z. Zgierski , J. Chem. Phys. 1978 , **69** , 5496 – 5508 . 15c. R. Englman , J. Jortner , Mol. Phys. 1970 , **18** , 145 – 164 .